Guided wave propagation and mode differentiation in hollow cylinders with viscoelastic coatings

Jing Mu and Joseph L. Rose[a)]
Department of Engineering Science and Mechanics, The Pennsylvania State University, University Park, Pennsylvania 16802

(Received 14 July 2007; revised 12 May 2008; accepted 14 May 2008)

Guided wave propagation theories have been widely explored for about one century. Earlier theories on single-layer elastic hollow cylinders have been very beneficial for practical nondestructive testing on piping and tubing systems. Guided wave flexural (nonaxisymmetric) modes in cylinders can be generated by a partial source loading or any nonaxisymmetric discontinuity. They are especially important for guided wave mode control and defect analysis. Previous investigations on guided wave propagation in multilayered hollow cylindrical structures mostly concentrate on the axisymmetric wave mode characteristics. In this paper, the problem of guided wave propagation in free hollow cylinders with viscoelastic coatings is solved by a semianalytical finite element (SAFE) method. Guided wave dispersion curves and attenuation characteristics for both axisymmetric and flexural modes are presented. Due to the fact that dispersion curve modes obtained from SAFE calculations are difficult to differentiate from each other, a mode sorting method is established to distinguish modes by their orthogonality. Theoretical proof of the orthogonality between guided wave modes in a viscoelastic coated hollow cylinder is provided. Wave structures are also calculated and discussed in view of wave mechanics in multilayered cylindrical structures containing viscoelastic materials. © *2008 Acoustical Society of America.* [DOI: 10.1121/1.2940586]

PACS number(s): 43.40.At, 43.20.Mv, 43.20.Bi, 43.20.Ks [YHB] Pages: 866–874

I. INTRODUCTION

The work on wave propagation in bounded structures by Lamb (1917) and Rayleigh (1945), etc. in the early part of the last century sparked the beginning of research on guided waves theories. Ever since then, it has been recognized that there exists a lot more wave modes in free waveguide structures than those in a bulk medium (Graff, 1991; Rose, 1999). These guided wave modes are, in general, much more complex than bulk waves, as they have to satisfy the boundary conditions of the waveguides. Around the 1950s, accompanied with the rapid development of modern computers, there emerged a massive amount of studies on guided wave dispersion curve computations on multilayered structures. The two computational methods that have been widely used until now are the transfer matrix approach developed by Thomson (1950) and the global matrix method by Knopoff (1964). A good summary of these matrix techniques can be found in Lowe (1995). A common feature of these matrix techniques is that a root searching routine has to be established in order to find the roots in the wave number and frequency domain. If the structure contains viscoelastic material, then the root searching process has to be performed on both real and imaginary wave number domains for each frequency. This can possibly make the root searching process time consuming. Moreover, roots may be missed in the searching process at high frequency when two modes approach very close to each other or matrix size becomes larger (Shorter 2004).

In 1959, Gazis obtained the complete solution for harmonic guided wave modes propagating in an infinite hollow cylinder. This has been very beneficial for long range guided wave inspection on widely distributed pipelines. In practice, however, most of the pipelines used in industry are covered with viscoelastic coatings for various protection purposes. Therefore, the exploration of guided wave propagation in viscoelastic coated hollow cylinders becomes quite indispensable.

Due to the aforementioned computation difficulties encountered in matrix methods, theoretical calculation of the wave modes in hollow cylinders with viscoelatic coatings can be difficult. Some researchers have studied plate or plate-like structures with viscoelastic properties, e.g., Simonetti (2004) and Predoi *et al.* (2007). These plate solutions may be safely used to approximate hollow cylinders with a thickness to radius ratio less than 10% (Luo *et al.*, 2005). Therefore, it is still valuable to search for a complete solution to wave propagation in multilayered viscoelastic cylinders. The axisymmetric wave modes of such a structure have been provided by Barshinger and Rose (2004) using the global matrix method, but the flexural modes were not provided in their paper. Ma *et al.* (2006) investigated the fundamental torsional mode scattering from an axisymmetric sludge layer inside a pipe. In his study, the sludge layer is considered to be an elastic epoxy layer. Beard and Lowe (2003) used guided waves to inspect the integrity of rock bolts. They provided three lower order (circumferential order equals 1) flexural modes in their study at relatively low frequency range (less than 300 kHz). Therefore, to the authors' best knowledge, such a complete solution, including both axisymmetric and nonaxisymmetric modes (flexural modes with circumferential orders equal or larger than one) in multilayered hollow cylindrical structures covering a relative wide fre-

[a)]Electronic mail: jlresm@engr.psu.edu

 0001-4966/2008/124(2)/866/9/$23.00

quency range (up to mega Hertz), has never been reported in the literature before. To the authors' knowledge, there has been a lack of investigation on the characteristics of higher order flexural modes in viscoelastic multilayered hollow cylindrical structures. The flexural modes can be generated by any partial source loading or any nonaxisymmetric anomaly in a cylinder. The flexural modes have shown to be highly contributive in the analysis of source influence and guided wave mode control (e.g., focusing) in elastic hollow cylinders (Ditri and Rose 1992; Li and Rose 2001, 2002). Therefore, our goal in this paper is to understand and seek the complete solution to this problem using appropriate techniques. The semianalytical finite element method (SAFEM) was developed as an alternative way to tackle the wave propagation problem. Early employment of SAFEM in solving guided wave propagation problems can be found in Nelson *et al.* (1971) and Dong and Nelson *et al.* (1972). In recent years, SAFEM was also applied to the analysis of wave modes across a pipe elbow (Hayashi *et al.*, 2005) and in materials with viscoelastic properties (Shorter, 2004; Bartoli *et al.*, 2006).

In this paper, SAFEM is adopted to generate phase velocity and attenuation dispersion curves including both axisymmetric and flexural modes in hollow cylinders with viscoelastic coatings. Modal characteristics, such as wave structures and attenuation properties are provided and discussed. Further, driven by the fact that the wave modes obtained from SAFE calculations are difficult to differentiate from each other, a mode sorting algorithm based on modal orthogonality is accomplished. An orthogonality relation based upon SAFE formulation for elastic waveguides is developed by Damljanović and Weaver (2004). Different from Damljanović and Weaver, the orthogonality relation derived in this study is valid for both elastic and viscoelastic materials. It can be used in either single-layered or multilayered cylindrical structures. It is applicable not only for dispersion curves calculation by SAFE formulations but also for those obtained from analytical derivations.

II. SAFE FORMULATION

Let us start with the governing equation provided by the virtual work principle for a free hollow cylinder with as in Hayashi *et al.* (2003) and Sun (2004). Only linear elastic and viscoelastic material behaviors are considered here:

$$\int_V \delta\mathbf{u}^T \cdot \rho\ddot{\mathbf{u}}\, dV + \int_V \delta\boldsymbol{\varepsilon}^T \cdot \boldsymbol{\sigma}\, dV = 0, \tag{1}$$

where T represents matrix transpose, ρ is density, and $\ddot{\mathbf{u}}$ is the second derivative of displacement $\mathbf{u}$ with respect to time t. $\int_V dV$ is the volume integrals of the element, respectively. In cylindrical coordinates, $dV = r\, dr\, d\theta\, dz$. The first and second terms on the left-hand side are the corresponding increment of kinetic energy and potential energy.

Sun (2004) used two-dimensional (2D) SAFE to calculate the flexural modes in a single elastic cylinder. He meshed the cross section of the cylinder in both thickness direction r and circumferential direction θ. In this study, we incorporate the solution $e^{in\theta}$ in the circumferential direction, so that we can use exact representations in both the θ and z directions. The finite element approximation reduces to only one dimension r. This does not only improves the accuracy in the calculation for flexural modes with higher circumferential orders, but also reduces computation cost. For a harmonic wave propagating in the z direction, the displacement at any point $\mathbf{u}(r,\theta,z,t)$ can be represented by

$$\mathbf{u}(r,\theta,z,t) = \sum_{j=1}^{2} \mathbf{N}(r)\mathbf{U}^j e^{i(kz+n\theta-\omega t)}, \tag{2}$$

where $\mathbf{U}^j$ is the nodal displacement vector at the jth element and $\mathbf{N}(r)$ is the shape function in the thickness direction r. For a two-node element, $\mathbf{U}^j$ is a six-element vector and $\mathbf{N}(r)$ is a 3×6 matrix. The shape function matrix is chosen as follows:

$$\mathbf{N} = \begin{bmatrix} N_1 & 0 & 0 & N_2 & 0 & 0 \\ 0 & N_1 & 0 & 0 & N_2 & 0 \\ 0 & 0 & N_1 & 0 & 0 & N_2 \end{bmatrix}, \tag{3}$$

with

$$N_1 = \tfrac{1}{2}(1-\xi), \quad N_2 = \tfrac{1}{2}(1+\xi), \tag{4}$$

where $-1 \leqslant \xi \leqslant 1$ is the natural coordinates in the r direction.

Substituting Eqs. (2)–(4) into Eq. (1), one obtains Eq. (5) after simplification:

$$(\mathbf{K}_1^j + ik\mathbf{K}_2^j + k^2\mathbf{K}_3^j)\mathbf{U}^j - \omega^2\mathbf{M}^j\mathbf{U}^j = 0. \tag{5}$$

In Eq. (5), we have

$$\mathbf{B}_1 = \begin{bmatrix} \frac{\partial N_1}{\partial r} & 0 & 0 & \cdots & & \\ \frac{N_1}{r} & i\frac{n}{r}N_1 & 0 & & & \\ 0 & 0 & 0 & & & \\ 0 & 0 & i\frac{n}{r}N_1 & \cdots & N_2 & \cdots \\ 0 & 0 & \frac{\partial N_1}{\partial r} & & & \\ i\frac{n}{r}N_1 & \frac{\partial N_1}{\partial r} - \frac{N_1}{r} & 0 & \cdots & & \end{bmatrix}_{6\times 6}, \tag{6}$$

$$\mathbf{B}_2 = \begin{bmatrix} 0 & 0 & 0 & 0 & 0 & 0 \\ 0 & 0 & 0 & 0 & 0 & 0 \\ 0 & 0 & N_1 & 0 & 0 & N_2 \\ 0 & N_1 & 0 & 0 & N_2 & 0 \\ N_1 & 0 & 0 & N_2 & 0 & 0 \\ 0 & 0 & 0 & 0 & 0 & 0 \end{bmatrix}_{6\times 6}, \tag{7}$$

$$\mathbf{K}_1^j = \int_r \int_\theta \mathbf{B}_1^T \mathbf{C} \mathbf{B}_1 r \, dr \, d\theta,$$

$$\mathbf{K}_2^j = \int_r \int_\theta (\mathbf{B}_1^T \mathbf{C} \mathbf{B}_2 - \mathbf{B}_2^T \mathbf{C} \mathbf{B}_1) r \, dr \, d\theta, \tag{8}$$

$$\mathbf{K}_3^j = \int_r \int_\theta \mathbf{B}_2^T \mathbf{C} \mathbf{B}_2 r \, dr \, d\theta,$$

$$\mathbf{M}^j = \rho \int_r \int_\theta \mathbf{N}^T \mathbf{N} r \, dr \, d\theta,$$

and $\mathbf{C}$ is the stiffness matrix.

Assembling Eq. (5) for all elements in the cross-sectional area, the equation for the whole system can be written as

$$(\mathbf{K}_1 + ik\mathbf{K}_2 + k^2\mathbf{K}_3)\mathbf{U} - \omega^2 \mathbf{M}\mathbf{U} = \mathbf{f}, \tag{9}$$

where $\mathbf{K}_1$, $\mathbf{K}_2$ $\mathbf{K}_3$, and $\mathbf{M}$ are the $M \times M$ matrices where M equals three times the number of nodes. In order to decrease the order of k, Eq. (9) can be further reformulated as

$$[\mathbf{A} - k\mathbf{B}]\mathbf{Q} = 0, \tag{10}$$

where

$$\mathbf{A} = \begin{bmatrix} 0 & \mathbf{K}_1 - \omega^2 \mathbf{M} \\ \mathbf{K}_1 - \omega^2 \mathbf{M} & i\mathbf{K}_2 \end{bmatrix},$$

$$\mathbf{B} = \begin{bmatrix} \mathbf{K}_1 - \omega^2 \mathbf{M} & 0 \\ 0 & -\mathbf{K}_3 \end{bmatrix},$$

$$\mathbf{Q} = \begin{bmatrix} \mathbf{U} \\ k\mathbf{U} \end{bmatrix}.$$

At a given frequency ω, the wave number k can be obtained by solving the eigenvalue problem in Eq. (10) using a standard eigenvalue routine. Then, the phase velocity and attenuation dispersion curves can be calculated from the real and imaginary parts of k. The corresponding wave structure $\mathbf{U}$ can be obtained from the upper half of the eigenvector $\mathbf{Q}$.

III. ORTHOGONALITY AND MODE SORTING

A common difficulty in producing dispersion curves calculated from the SAFE formulation is modal differentiation. Modal differentiation is tremendously helpful to interpret the behaviors of different modes. It also forms the basis of solving such further problems as wave scattering, source influence, and mode control. Of particular importance in mode sorting is to find the distinctive characteristics between different modes. A natural way of realizing this is to utilize the modal orthogonality, which is an intrinsic law followed by all guided wave modes. Damljanović and Weaver (2004) presented an orthogonality relation based on SAFE formulation for elastic waveguides and used it to solve a point source loading problem. Loveday and Long (2007) also employed this relation to sort the guided wave modes in a rail. Another way of sorting wave modes can be realized by identifying the similarity between wave modes at adjacent frequencies. However, we prefer to using orthogonality here not only due to the fact that orthogonality is a natural attribute of guided wave modes, but also because mode sorting based on orthogonality can help future research on wave scattering and source influence in multilayered cylinders.

The analytical orthogonality relations have been studied and used by researchers for decades. The orthogonality relation for the Rayleigh–Lamb modes of a 2D plate was obtained by Fraser (1976). Later, orthogonality relations of guided wave modes have been used as a powerful tool in the study of wave scattering (Kino, 1978; Engan, 1998; Shkerdin and Glorieux, 2004, 2005; Vogt *et al.*, 2003) and source influence (Ditri and Rose, 1992, 1994) analysis. In these studies, orthogonality relations are derived from either real or complex reciprocity relations. As has been pointed out by Auld (1990), both real and complex reciprocity relations are valid for elastic waveguides. If we set out from the real reciprocity relation, we will reach an orthogonality relation stating that the mode is orthogonal to all the other modes except a mode with the same modal behavior, but incoming from the opposite propagating direction, which is the case in this paper. On the other hand, starting out from the complex reciprocity relation yields an orthogonality relation stating that the mode is orthogonal to all the other modes except itself. Like the two reciprocity relations, these two types of orthogonality relations are both valid for elastic waveguides. However, only the real reciprocity relation is valid for viscoelastic materials and our purpose is to obtain an orthogonality relation that is applicable for viscoelastic waveguides. Thus, it is necessary to build the orthogonality relation base on the real reciprocity relation. The utilization of orthogonality relations is associated with guided wave modes and, therefore, is dependent on waveguide geometries. For example, to solve the source influence problem in hollow cylinders, the reciprocity relation formulated in three-dimensional (3D) cylindrical coordinates has to be used, whereas a reciprocity relation formulated in a 2D Cartesian coordinated may be used to analyze the wave field in a plate. The orthogonality relations for 3D solid cylinders and hollow cylinders have been provided by Vogt *et al.* (2003), Engan (1998), and Ditri and Rose (1992) by using the stress free boundary conditions under cylindrical coordinates. Here, for a multilayered viscoelastic cylinder, we show that the orthogonality relation is still valid by taking into account both the interface continuity conditions and stress free boundary conditions.

In this section, the analytical derivation of orthogonality of the modes in multilayered cylindrical structures containing both elastic and viscoelastic materials will be given. Different from the orthogonality relation developed by Damljanović and Weaver (2004), the orthogonality developed in this paper can be applied to multilayered waveguides containing any combination of elastic and viscoelastic materials. In addition, as the following orthogonality relation is derived analytically, it can be applied to dispersion curves obtained from either the SAFE formulation or from the matrix methods. In the following, the mode sorting process will be discussed accordingly.

Before we get started, it is worthwhile to introduce the notation used in the derivation to represent guided wave modes in cylindrical structures. Overall, we follow the notations used in Ditri and Rose (1992). Guided wave modes in a cylindrical waveguide can be represented by two indices, e.g., $T(m,n)$ or $L(m,n)$, where $m \in \{0,1,2,\ldots\}$ is the index of circumferential order, $n \in \{1,2,\ldots\}$ is the nth root of the characteristic equation of circumferential order m for torsional type (denoted by T) and longitudinal type (denoted by L) of the mode, respectively. Conventionally, modes with the same circumferential order m are often called a mode group or a mode family. In this paper, a mode group or family refers to longitudinal or torsional types of modes of the same n but with different circumferential orders. The reason to do this lays in the fact that longitudinal or torsional types of modes with the same n, but different circumferential orders, bear similar modal characteristics, such as phase velocities, attenuation, and wave structures in the thickness direction.

The orthogonality of normal modes in an elastic hollow cylinder was first developed by (Ditri and Rose 1992). The orthogonality of normal modes in multilayered hollow cylinders containing viscoelastic materials can be derived in a similar manner. Therefore, the derivation procedure will only be given briefly here. Let us start with the real reciprocity relation (Auld 1990)

$$\nabla \cdot (\mathbf{v}_1 \cdot \mathbf{T}_2 - \mathbf{v}_2 \cdot \mathbf{T}_1) = 0, \tag{11}$$

where $\mathbf{v}_1$, $\mathbf{v}_2$ and $\mathbf{T}_1$, $\mathbf{T}_2$ are the particle velocities and stresses for two different wave modes (either torsional or longitudinal type) in a multilayered hollow cylinder. Without loss of generality, $\mathbf{v}_1$, $\mathbf{v}_2$ and $\mathbf{T}_1$, $\mathbf{T}_2$ can be represented as

$$\mathbf{v}_1 = \mathbf{v}_m^N e^{-i\beta_m^N z}, \quad \mathbf{T}_1 = \mathbf{T}_m^N e^{-i\beta_m^N z}, \tag{12}$$

$$\mathbf{v}_2 = \mathbf{v}_n^M e^{-i\beta_n^M z}, \quad \mathbf{T}_2 = \mathbf{T}_n^M e^{-i\beta_n^M z}, \tag{13}$$

where N and M are circumferential orders, n and m are indices of mode group, and β denotes the wave number of mode (M,n) or (N,m).

Substituting the previous expressions for $\mathbf{v}_1$, $\mathbf{v}_2$ and $\mathbf{T}_1$, $\mathbf{T}_2$ into Eq. (11) yields

$$\nabla_{r\theta} \cdot (\mathbf{v}_m^N \cdot \mathbf{T}_n^M - \mathbf{v}_n^M \cdot \mathbf{T}_m^N) - i(\beta_m^N + \beta_n^M)(\mathbf{v}_m^N \cdot \mathbf{T}_n^M - \mathbf{v}_n^M \cdot \mathbf{T}_m^N) \cdot \hat{\mathbf{e}}_z = 0, \tag{14}$$

where $\nabla_{r\theta}$ is the 2D divergence operator in cylindrical coordinates. By integrating both sides of Eq. (14) over the cross section D of the viscoelastic coated hollow cylinder, we obtain

$$\iint_D \nabla_{r\theta} \cdot (\mathbf{v}_m^N \cdot \mathbf{T}_n^M - \mathbf{v}_n^M \cdot \mathbf{T}_m^N) d\sigma = -4i(\beta_m^N + \beta_n^M) P_{mn}^{NM}, \tag{15}$$

where

$$P_{mn}^{NM} = -\frac{1}{4} \iint_D (\mathbf{v}_m^N \cdot \mathbf{T}_n^M - \mathbf{v}_n^M \cdot \mathbf{T}_m^N) \cdot \hat{\mathbf{e}}_z d\sigma. \tag{16}$$

By applying the Gauss divergence theorem to the left-hand side of Eq. (15), we have

$$\begin{aligned} \iint_D \nabla_{r\theta} \cdot (\mathbf{v}_m^N \cdot \mathbf{T}_n^M - \mathbf{v}_n^M \cdot \mathbf{T}_m^N) d\sigma = & \oint_{\partial_1 D} (\mathbf{v}_m^N \cdot \mathbf{T}_n^M - \mathbf{v}_n^M \cdot \mathbf{T}_m^N) \cdot \hat{\mathbf{n}}_1 ds + \oint_{\partial_2 D} (\mathbf{v}_m^N \cdot \mathbf{T}_n^M - \mathbf{v}_n^M \cdot \mathbf{T}_m^N) \cdot \hat{\mathbf{n}}_2 ds \\ & + \oint_{\partial_2 D} (\mathbf{v}_m^N \cdot \mathbf{T}_n^M - \mathbf{v}_n^M \cdot \mathbf{T}_m^N) \cdot \hat{\mathbf{n}}_1 ds + \oint_{\partial_3 D} (\mathbf{v}_m^N \cdot \mathbf{T}_n^M - \mathbf{v}_n^M \cdot \mathbf{T}_m^N) \cdot \hat{\mathbf{n}}_2 ds, \end{aligned} \tag{17}$$

where $\partial_1 D$ represents the inner boundary of the cross section of the elastic hollow cylinder, $\partial_2 D$ represents the interface between the cross sections of the elastic hollow cylinder and the viscoelastic coating, and $\partial_3 D$ represents the outer boundary of the cross section of the viscoelastic coating. The unit vectors $\hat{\mathbf{n}}_1$ and $\hat{\mathbf{n}}_2$ are defined as

$$\hat{\mathbf{n}}_1 = -\hat{\mathbf{r}}, \quad \hat{\mathbf{n}}_2 = \hat{\mathbf{r}}. \tag{18}$$

By using the fact that the displacements and normal stresses are continuous at the interface $\partial_2 D$, Eq. (17) can be simplified to

$$\begin{aligned} \iint_D \nabla_{r\theta} \cdot (\mathbf{v}_m^N \cdot \mathbf{T}_n^M - \mathbf{v}_n^M \cdot \mathbf{T}_m^N) d\sigma = & \oint_{\partial_1 D} (\mathbf{v}_m^N \cdot \mathbf{T}_n^M - \mathbf{v}_n^M \cdot \mathbf{T}_m^N) \cdot \hat{\mathbf{n}}_1 ds + \oint_{\partial_3 D} (\mathbf{v}_m^N \cdot \mathbf{T}_n^M - \mathbf{v}_n^M \cdot \mathbf{T}_m^N) \cdot \hat{\mathbf{n}}_2 ds. \end{aligned} \tag{19}$$

Further, by noticing that the tractions produced by the modes (M,n) and (N,m) vanish at the free boundaries of the waveguides for the right-hand side of Eq. (19), we obtain

$$\iint_D \nabla_{r\theta} \cdot (\mathbf{v}_m^N \cdot \mathbf{T}_n^M - \mathbf{v}_n^M \cdot \mathbf{T}_m^N) d\sigma = 0. \tag{20}$$

Combining Eqs. (15) and (20), we acquire

$$P_{mn}^{NM} = 0, \quad \beta_m^N \neq -\beta_n^M. \tag{21}$$

In addition to Eq. (21), direct evaluation of P_{mn}^{NM} using the orthogonality of the angular eigenfunctions $\cos(N\theta)$, $\sin(M\theta)$, etc. provides us with the orthogonality relation in multilayered hollow cylinders containing viscoelastic materials

$$P_{mn}^{NM} = 0, \quad \text{for } M \neq N \text{ or } \beta_m^N \neq -\beta_n^M. \tag{22}$$

Once the orthogonality relation is obtained, guided modes can be sorted by calculating P_{mn}^{NM} between the modes of adjacent frequencies. For instance, solving Eq. (10) yields N_1 modes at frequency ω_1 and N_2 modes at the adjacent frequency ω_2, where $\omega_2 - \omega_1 = \Delta\omega$ is the frequency step. P_{mn}^{NM} is then calculated between each mode at ω_2 and all of the modes at ω_1 using Eq. (17) to obtain N_1 results. The biggest value in the N_1 results indicates the two modes used for this orthogonality calculation belonging to the same mode in the dispersion curves. In fact, the other values will be very close to zero. Here, we do not have to know the values of m, n, and M, N. We only need to utilize the wave structures obtained from Eq. (10) for the two modes under concern, calculate

TABLE I. Material properties.

Material	C_L (mm/μs)	$\frac{\alpha_L}{\omega}$ (μs/mm)	C_S (mm/μs)	$\frac{\alpha_S}{\omega}$ (μs/mm)	ρ (g/cm^3)
Steel	5.85	⋯	3.23	⋯	7.86
E&C 2057/ Cat9 expoxy	2.96	0.0047	1.45	0.0069	1.6
Bitumastic 50	1.86	0.023	0.75	0.24	1.5

their corresponding stress components, and input these stress and displacement components into Eq. (16) to calculated P_{mn}^{NM}. It can be seen from this procedure that the orthogonality computation is performed $N_1 \times N_2$ times for the two adjacent frequencies. Strictly speaking, the orthogonality relation in Eq. (22) is valid among the modes under any single arbitrary frequency. However, we are performing it between two adjacent frequencies ω_1 and ω_2 as an approximation. As the behavior of the wave modes in the dispersion curves varies continuously, this approximation holds well for relatively small frequency steps. The frequency step used in our calculation is 10 kHz and the mode sorting procedure worked effectively.

IV. NUMERICAL RESULTS

A. Low attenuative material: E&C 2057 Cat9 expoxy

In order to verify our calculation, the dispersion curves for a 4 in. schedule 40 steel hollow cylinder coated with 0.02 in. E&C 2057 / Cat9 expoxy are calculated and compared with previous axisymmetric results given by Barshinger and Rose (2004). Nevertheless, the formulation provided in this paper is general. It is applicable to other pipe sizes and other viscoelastic and elastic cylinders. The materials that can be used in analytical matrix method can also be implemented in our calculations. It is simply a different input for material and pipe size, the solving procedure is the same. Even more complex material properties, for example, experimental material properties varying nonlinearly with frequency can be easily implemented. However, this is beyond the scope of this paper and will not be addressed in detail here. The numbers of elements used in our calculation for the elastic and viscoelastic layers are 24 and 4, respectively. The material properties are listed in Table I, where C_L and C_S are the longitudinal and shear bulk wave velocities, respectively. The terms α_L and α_S are attenuation parameters associated with longitudinal and shear bulk waves. They are frequency dependent. The viscoelastic material properties are experimentally measured. Details can be found in Barshinger (2001). Based on the correspondence principle (Christensen, 1981), wave propagation problems in elastic materials can be converted to those in viscoelastic materials by simply using complex material parameters. This makes the SAFE calculations for both elastic and viscoelastic cases essentially the same, except that the input parameters are different.

The dispersion curves of the longitudinal mode group (denoted by L) and the torsional mode group (denoted by T) after mode sorting for axisymmetric (circumferential order n equals zero) and flexural modes (circumferential order n ranges from one to ten) are plotted in Figs. 1 and 2, respectively. For clarity, a magnified inset for wave attenuation at low frequencies (below 300 kHz) is also shown in Fig. 2. In Figs. 1 and 2, the different modes are lined up very well with respect to frequency. Mode sorting can be very helpful when using guided wave modes. Especially when the number of wave modes is big (e.g., more than 20 modes), there may be

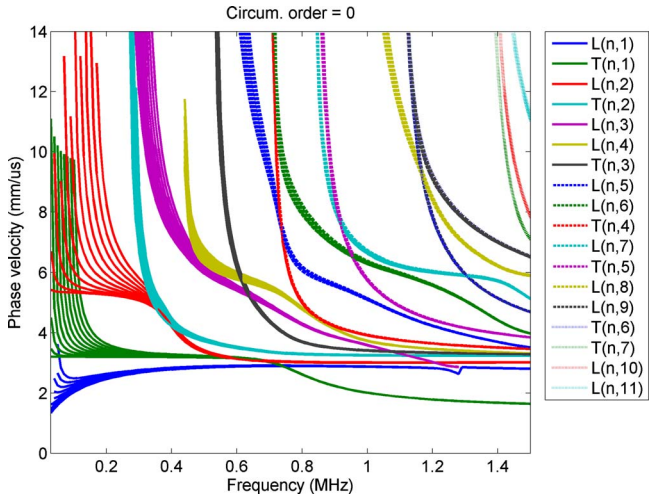

FIG. 1. (Color online) Phase velocity dispersion curves for guided wave modes with circumferential order n from 0 to 10 in a 4 in. schedule 40 steel hollow cylinder coated with 0.02 in. thick E&C 2057 Cat9 expoxy.

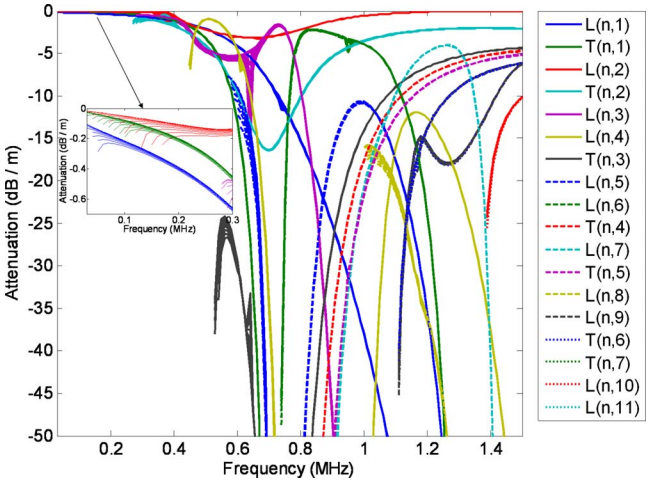

FIG. 2. (Color online) Attenuation dispersion curves for guided wave modes with circumferential order n from 0 to 10 in a 4 in. schedule 40 steel hollow cylinder coated with 0.02 in. thick E&C 2057 Cat9 expoxy.

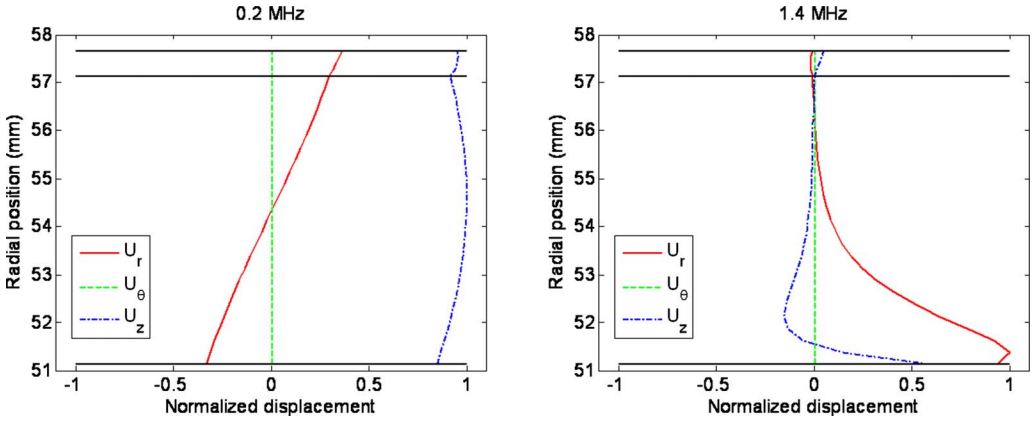

FIG. 3. (Color online) Normalized displacement distribution across hollow cylinder thickness for the L(0,2) mode at 0.2 and 1.4 MHz.

multiple mode crossings or mode branches, which makes it difficult to identify the trend of a specific mode under investigation. Our next example on highly attenuative material will illustrate this aspect even better. For well sorted wave modes, it will be very convenient to analyze the behavior of a specific mode with respect to frequency. On one hand, the orthogonality between different modes in natural waveguides provides us with a natural way of mode sorting. On the other hand, mode sorting can also serve as an effective means of verifying the above derivation and calculation of dispersion curves. The results in Figs. 1 and 2 validated our theory of orthogonality. This orthogonality mode sorting method is a powerful tool and can be applied to various waveguides such as multilayered plates, beams, rods, rails, and so on.

It can be seen from Fig. 2 that guided wave attenuation is majorly nonmonotonic with an increase in frequency. However, if observed carefully, several characteristics can be noticed: (1) The most striking characteristic in Fig. 2 is that the mode group $L(n,2)$ has low attenuation in almost the whole frequency bandwidth. Especially for frequency higher than 1.2 MHz, the attenuation of the mode group $L(n,2)$ converges to zero asymptotically. (2) The attenuation of mode groups $L(n,1)$ and $T(n,1)$ increases monotonically with an increase in frequency. The attenuations with these modes below 0.2 MHz are less than 1 dB/m. As a result, the two wave groups in this region are good choices in nondestructive testing. (3). Generally speaking, for almost all of the other mode groups having cutoff frequencies in the corresponding bare hollow cylinder problem, very high attenuation occurs close to their cutoff frequencies. This makes sense, as they become nonpropagating modes for frequencies lower than their cutoff frequencies in a hollow cylinder without viscoelastic coatings. As the frequency increases, the attenuation (the absolute value of attenuation in Fig. 2) decreases and reaches its minimum at a certain frequency for a certain mode. After that, the attenuation increases again with an increase of frequency. This is a significant characteristic as it occurs for almost all of the wave modes. Finding out where the minimal attenuation values occur for the different wave modes is crucial for nondestructive evaluation applications and would be an interesting subject for future work.

For comparison purposes, the phase velocity and attenuation dispersion curves for axisymmetric longitudinal and torsional modes are also calculated from the analytical formulation developed in Barshinger and Rose (2004). It is found that the longitudinal and torsional dispersion curves generated from the analytical matrix method match the axisymmetric results in Figs. 1 and 2 very well. However, the computational cost of the SAFE method is less even with the mode sorting procedure incorporated. For brevity, these comparison results will not be shown in this paper.

Wave structures are displacement amplitude distributions along the thickness direction for certain guided wave modes. The behavior of a specific guided wave mode is highly related to its wave structure. From the previous analysis regarding the phase velocity and attenuation dispersion curves, it is natural to consider the mode group $L(n,2)$ of most interest, since this group is the least attenuative at both low ($<$0.32 MHz) and high ($>$1 MHz) frequencies. Sample wave structures of $L(0,2)$ (axisymmetric mode) and $L(5,2)$ (flexural mode) at 0.2 and 1.4 MHz are shown in Figs. 3 and 4, respectively. The coated hollow cylinder size and material parameters are the same as those used in the dispersion curve calculations.

It can be seen that the wave structure of $L(0,2)$ at low frequency (0.2 MHz) has a similar distribution as the S0 mode in plate. The wave structure changes with frequency. At a frequency of 1.4 MHz, the wave structure of $L(0,2)$ changes to become similar to that of a surface wave. In addition, the displacement is mostly concentrated on the inner surface of the two layered hollow cylinder. This phenomenon explains why the attenuation of $L(0,2)$ approaches zero at high frequencies. Comparison of wave structures from $L(0,2)$ and $L(5,2)$ reveals that the displacements in the radial and axial directions (U_r and U_z) have very similar distributions for axisymmetric modes and flexural modes in a mode group. However, the displacements in the circumferential direction for $L(0,2)$ and $L(5,2)$ are similar at high frequency but different at low frequency. This can be expected because the wave velocities of the modes with different circumferential orders in a mode group are quite different at low frequency, but approach each other at high frequency.

From the earlier discussion, it can be seen that wave mode attenuation in a multilayered hollow cylinder is highly related to its energy concentration in the viscoelastic layer.

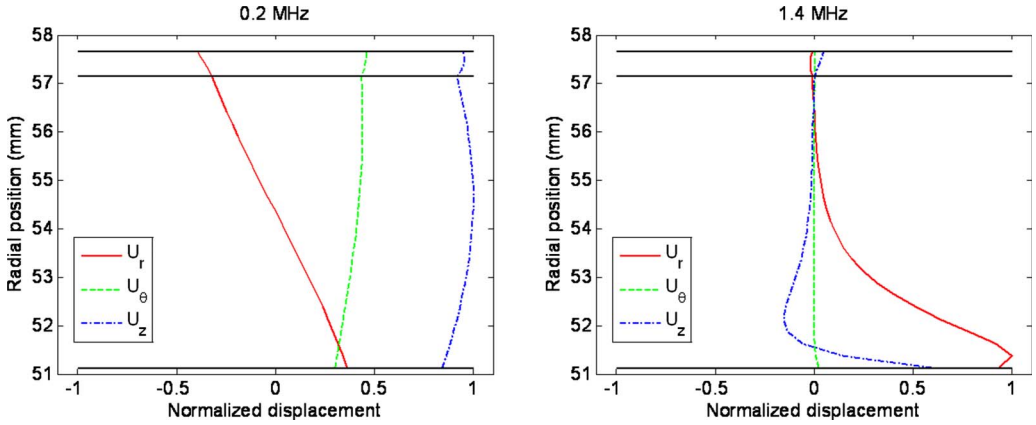

FIG. 4. (Color online) Normalized displacement distribution across hollow cylinder thickness for the L(5,2) mode at 0.2 and 1.4 MHz.

The more the energy is concentrated in the viscoelastic layer, the greater the attenuation for the wave mode. This conclusion is also drawn in Simonetti (2004) to approximate the guided wave attenuation by calculating the portion of energy contained in the viscoelastic layer of a multilayered plate structure.

B. Highly attenuative material: Bitumastic 50

The properties of Bitumastic 50 (Barshinger and Rose, 2004) are also given in Table I. It can be seen from Table I that Bitumastic 50 is much more attenuative, especially for shear waves, compared to E&C 2057/Cat9 epoxy.

The phase velocity dispersion curves and attenuation curves for a 4 in. schedule 40 steel pipe coated with 0.02 in Bitumastic 50 are calculated and shown in Figs. 5 and 6. A threshold is set for displaying the dispersion curves, so that the modes with an imaginary part of a wave number larger than 0.5 are not shown in Fig. 6. Comparing the phase velocity dispersion curves in Fig. 5 to those in Fig. 1, two major features can be observed in Fig. 5. First, the phase velocities of certain modes groups $L(n,3)$ and $L(n,6)$ decrease at their low frequencies. Second, at relatively high frequencies, some modes experience nonmonotonic variation with the increase of frequency, e.g., modes $L(n,3)$ and $L(n,5)$ in the circled areas B and A. Nonmonotonic change of phase velocity with frequency is also found in the dispersion curves of highly attenuative plates (Chan and Cawley, 1998). It is pointed out in the paper that the rising in phase velocity with the increase in frequency may be associated with the amplitude ratio between the longitudinal and shear partial waves in the waveguide.

Figure 6 shows the wave modes whose attenuations are smaller than 100 dB/m. A comparison between the attenuation curves in Figs. 2 and 6 reveals that, overall, the mode groups in a 4 in. schedule 40 pipe coated with Bitumastic 50 are more attenuative than the same mode groups in a 4 in. schedule 40 pipe but coated with E&C 2057/Cat9 epoxy of the same thickness. This agrees with the material properties of the two coatings.

Figure 7 shows the magnified axisymmetric phase velocity dispersion curves in the circled area A in Fig. 5. The modal behavior in this region is relatively more complex compared to that in the other regions. In Fig. 7, several modes cross each other and mode $L(0,5)$ changes nonmonotonically with the increase of frequency. Eight points are chosen on the three guided wave modes shown in Fig. 7, they are labeled A–H. The detailed information of the chosen modes including frequency, phase velocity values, and at-

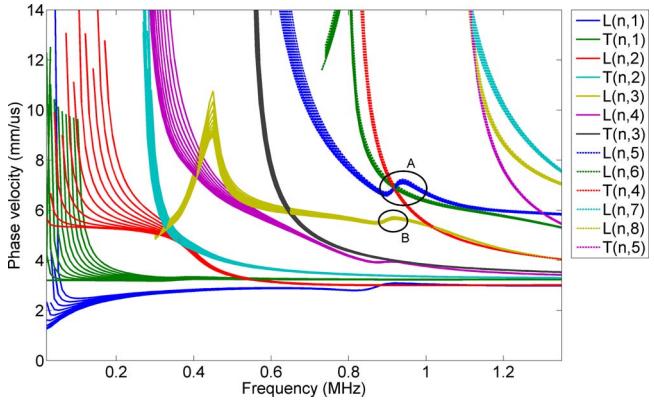

FIG. 5. (Color online) Phase velocity dispersion curves for guided wave modes with circumferential order n from 0 to 10 in a 4 in. schedule 40 steel hollow cylinder coated with 0.02 in. thick Bitumastic 50.

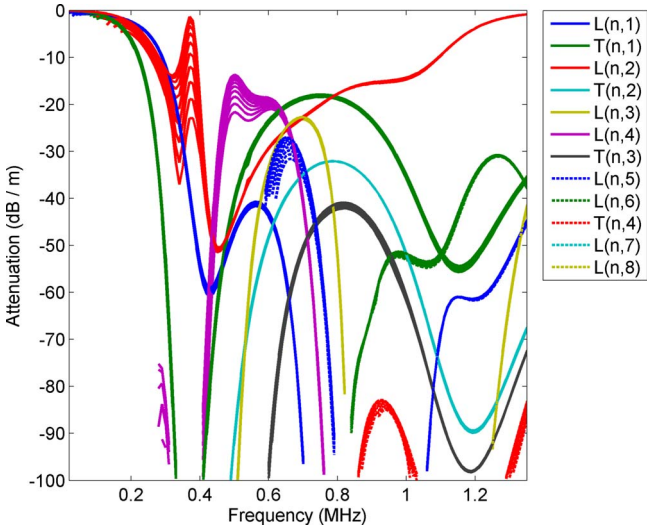

FIG. 6. (Color online) Attenuation curves for guided wave modes with circumferential order n from 0 to 10 in a 4 in. schedule 40 steel hollow cylinder coated with 0.02 in. thick Bitumastic 50.

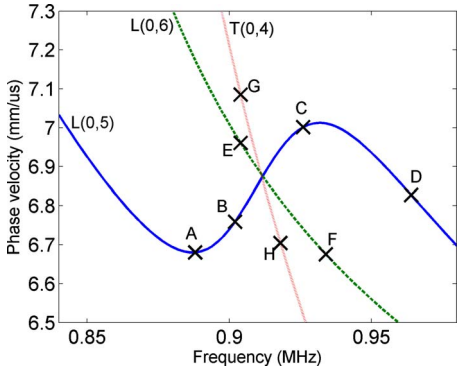

FIG. 7. (Color online) Magnified axisymmetric phase velocity dispersion curves in the circled area A in Fig. 5.

tenuation values are listed in Table II. It may be noticed from Table II that the attenuation values of mode $L(0,5)$ at points A, B, and C are much higher than the attenuation at point D. An inspection of the other modals reveals that the modes are generally more attenuative at the regions where phase velocity rising with the increase in frequency than the surrounding regions. The wave structures of the four points A to D on the mode $L(0,5)$ are plotted in Fig. 8. It can be clearly seen from Fig. 8 that the four wave structures are very similar to each other, which verifies that they are from the same mode and the mode $L(0,5)$ does evolve nonmonotonically with frequency in this region. Further investigation on modes $L(0,6)$ and $T(0,4)$ also reveals that the mode sorting in accurate in this region.

TABLE II. List of selected modes.

Label	Mode	Frequency (MHz)	Phase velocity (mm/μs)	Attenuation (dB/m)
A	L(0,5)	0.888	6.6802	−698.95
B	L(0,5)	0.902	6.7590	−875.21
C	L(0,5)	0.926	7.001	−797.84
D	L(0,5)	0.964	6.8276	−392.48
E	L(0,6)	0.904	6.9608	−71.052
F	L(0,6)	0.934	6.6752	−62.535
G	T(0,4)	0.904	7.0852	−98.064
H	T(0,4)	0.918	6.7044	−98.052

V. CONCLUSION

In this paper, the phase velocity and attenuation dispersion curves for a hollow cylinder with viscoelastic coating are developed by a SAFE formulation. It is analytically shown that the guided wave modes in such a multilayered cylinder containing viscoelastic materials are normal modes with orthogonality relations. Similar orthogonality relations can also be expected in various waveguides such as multilayered plates, rods, and rails. A mode sorting method based upon the orthogonality of normal modes is applied to the dispersion curves and excellent mode sorting results are obtained. The mode sorting results also validate the orthogonality relation. Numerical results are given to two different kinds of viscoelastic coating materials to verify the theoretical derivations and explore wave propagation characteristics in each case. Dispersion curves and sample wave structures are pro-

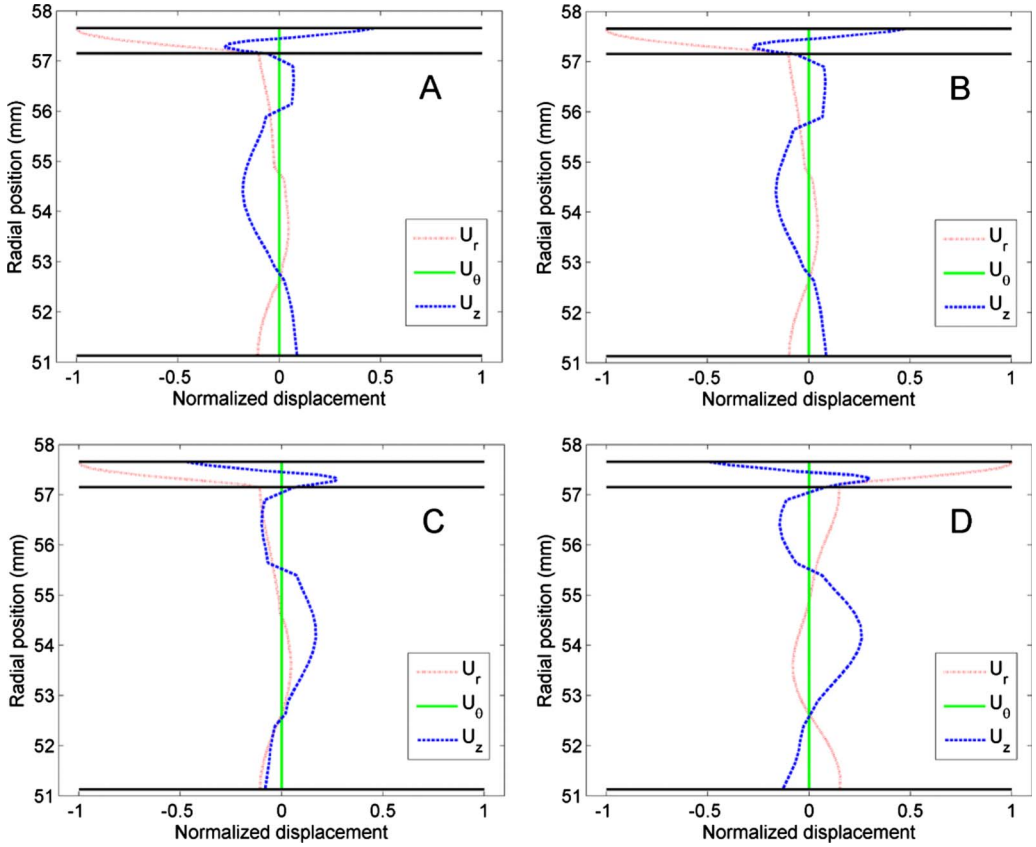

FIG. 8. (Color online) Wave structures of A, B, C, and D on mode L(0,5) in Fig. 7.

vided and the relation between wave structures and attenuation characteristics for flexural modes are discussed.

Auld, B. A. (**1990**). *Acoustic fields and waves in solids*, 2nd ed. (Krieger, Malabar, FL), Vol. **II**, pp. 153–154.

Barshinger, J. N. (**2001**). "Guided wave propagation in pipes with viscoelastic coatings," Ph.D. thesis, The Pennsylvania State University.

Barshinger, J. N., and Rose, J. L. (**2004**). "Guided wave propagation in an elastic hollow cylinder coated with a viscoelastic material," IEEE Trans. Ultrason. Ferroelectr. Freq. Control **51**, 1547–1556.

Bartoli, I., Marzani, A., Lanza di Scalea, F., and Viola, E. (**2006**). "Modeling wave propagation in damped waveguides of arbitrary cross-section," J. Sound Vib. **295**, 685–707.

Beard, M. D., and Lowe, M. J. S. (**2003**). "Non-destructive testing of rock bolts using guided ultrasonic waves," Int. J. Rock Mech. Min. Sci. **40**, 527–536.

Chan, C. W., and Cawley, P. (**1998**). "Lamb waves in highly attenuative plastic plates," J. Acoust. Soc. Am. **104**, 874–881.

Christensen, R. M. (**1981**). *Theory of Viscoelasticity: An Introduction* (Academic, New York).

Damljanović, V., and Weaver, R. L. (**2004**). "Forced response of a cylindrical waveguide with simulation of the wavenumber extraction problem," J. Acoust. Soc. Am. **115**, 1582–1591.

Ditri, J. J., and Rose, J. L. (**1992**). "Excitation of guided elastic wave modes in hollow cylinders by applied surface tractions," J. Appl. Phys. **72**, 2589–2597.

Ditri, J. J., and Rose, J. L. (**1994**). "Excitation of guided waves in generally anisotropic layers using finite sources," J. Appl. Mech. **61**, 330–338.

Dong, S., and Nelson, R. (**1972**). "On natural vibrations and waves in laminated orthotropic plates," J. Appl. Mech. **39**, 739–745.

Engan, H. E. (**1998**). "Torsional wave scattering from a diameter step in a rod," J. Acoust. Soc. Am. **104**, 2015–2024.

Fraser, W. B. (**1976**). "Orthogonality relation for the Rayleigh-Lamb modes of vibration of a plate," J. Acoust. Soc. Am. **59**, 215–216.

Gazis, D. C. (**1959**). "Three dimensional investigation of the propagation of waves in hollow circular cylinders. I. Analytical foundation," J. Acoust. Soc. Am. **31**, 568–573.

Graff, K. F. (**1991**). *Wave Motion in Elastic Solids* (Dover, New York).

Hayashi, T., Kawashima, K., Sun, Z., and Rose, J. L. (**2005**). "Guided wave propagation mechaninics across a pipe elbow," J. Pressure Vessel Technol. **127**, 322–327.

Hayashi, T., Song, W.-J., and Rose, J. L. (**2003**). "Guided wave dispersion curves for a bar with an arbitrary cross-section, a rod and rail example," Ultrasonics **41**, 175–183.

Kino, G. S. (**1978**). "The application of reciprocity theory to scattering of acoustic waves by flaws," J. Appl. Phys. **49**, 3190–3199.

Knopoff, L. (**1964**). "A matrix method for elastic wave problems," Bull. Seismol. Soc. Am. **54**, 431–438.

Lamb, H. (**1917**). "On waves in an elastic plate," Proc. R. Soc. London, Ser. A **93**, 114-128.

Li, J., and Rose, J. L. (**2001**). "Excitation and propagation of nonaxisymmetric guided waves in a hollow cylinder," J. Acoust. Soc. Am. **109**, 457–464.

Li, J., and Rose, J. L. (**2002**). "Angular-profile tuning of guided waves in hollow cylinders using a circumferential phased array," IEEE Trans. Ultrason. Ferroelectr. Freq. Control **49**, 1720–1729.

Loveday, P. W., and Long, C. S. (**2007**). "Time domain simulation of piezoelectric excitation of guided waves in rails using waveguide finite elements," Proc. SPIE **6529**, 65290V.

Lowe, M. J. (**1995**). "Matrix techniques for modeling ultrasonic waves in multilayered media," IEEE Trans. Ultrason. Ferroelectr. Freq. Control **42**, 525–542.

Luo, W., Zhao, X., and Rose, J. L. (**2005**). "A guided wave plate experiment for a pipe," J. Pressure Vessel Technol. **127**, 345–350.

Ma, J., Simonetti, F., and Lowe, M. J. S. (**2006**). "Scattering of the fundamental torsional mode by an axisymmetric layer inside a pipe," J. Acoust. Soc. Am. **120**, 1871–1880.

Nelson, R. B., Dong, S. B., and Kalra, R. D. (**1971**). "Vibrations and waves in laminated orthotropic circular cylinders," J. Sound Vib. **18**, 429–444.

Predoi, M. V., Castaings, M., Hosten, B., and Bacon, C. (**2007**). "Wave propagation along transversely periodic structures," J. Acoust. Soc. Am. **121**, 1935–1944.

Rayleigh, J. (**1945**). *The Theory of Sound* (Dover, New York).

Rose, J. L. (**1999**). *Ultrasonic Waves in Solid Media* (Cambridge University Press, Cambridge).

Schwab, F. (**1970**). "Surface-wave dispersion computations: Knopoff's method," Bull. Seismol. Soc. Am. **60**, 1491–1520.

Shkerdin, G., and Glorieux, C. (**2004**). "Lamb mode conversion in a plate with a delamination," J. Acoust. Soc. Am. **116**, 2089–2100.

Shkerdin, G., and Glorieux, C. (**2005**). "Lamb mode conversion in an absorptive bi-layer with a delamination," J. Acoust. Soc. Am. **118**, 2253–2264.

Shorter, P. J. (**2004**). "Wave propagation and damping in linear viscoelastic laminates," J. Acoust. Soc. Am. **115**, 1917–1925.

Simonetti, F. (**2004**). "Lamb wave propagation in elastic plate coated with viscoelastic materials," J. Acoust. Soc. Am. **115**, 2041–2053.

Sun, Z. (**2004**). "Phased array focusing wave mechanics in tubular structures," Ph.D. thesis, The Pennsylvania State University.

Thomson, W. T. (**1950**). "Transmission of elastic waves through a stratified solid medium," J. Appl. Phys. **21**, 89–93.

Vogt, T., Lowe, M., and Cawley, P. (**2003**). "The scattering of guided waves in partly embedded cylindrical structures," J. Acoust. Soc. Am. **113**, 1258–1272.